Environmental Chemistry Letters (2021) 19:3967–3972
https://doi.org/10.1007/s10311-021-01300-0

ORIGINAL PAPER

Corona and polio viruses are sensitive to short pulses of W-band gyrotron radiation

Lukasz S. Kaczmarczyk[1,2] · Katherine S. Marsay[1] · Sergey Shevchenko[3] · Moritz Pilossof[3] · Nehora Levi[1,2] · Moshe Einat[3] · Matan Oren[1] · Gabi Gerlitz[1,2]

Received: 30 April 2021 / Accepted: 28 July 2021 / Published online: 25 August 2021

Abstract

The severe acute respiratory syndrome coronavirus 2 (SARS-CoV-2) pandemic has raised the need of versatile means for virus decontamination. Millimeter waves are used in biochemical research in dynamic nuclear polarization enhanced nuclear magnetic resonance (DNP/NMR) spectroscopy. However, their efficiency in object decontamination for viruses has not been tested yet. Here we report the high efficiency of 95 GHz waves in killing both coronavirus 229E and poliovirus. An exposure of 2 s to 95 GHz waves reduced the titer of these viruses by 99.98% and 99.375%, respectively, and formed holes in the envelope of 229E virions as detected by scanning electron microscopy (SEM) analysis. The ability of 95 GHz waves to reduce the coronavirus titer to a range of limited infective dose of SARS-CoV-2 for humans and animal models along with precise focusing capabilities for these waves suggest 95 GHz waves as an effective way to decontaminate objects.

Keywords Gyrotron · 95 GHz waves · Coronavirus · Disinfection · Sterilization · Viral inactivation

Introduction

In December 2019, an outbreak of life-threatening pneumonia occurred in the Hubei Province of China. The causative agent was identified as a novel betacoronavirus that was named severe acute respiratory syndrome coronavirus 2 (SARS-CoV-2) (Zhu et al. 2020). SARS-CoV-2 has spread over the world causing a severe pandemic (Atzrodt et al. 2020; Sallard et al. 2021). Handling the SARS-CoV-2 pandemic requires various means to prevent person-to-person virus spread (Dai et al. 2021). Transmission of SARS-CoV-2 is not completely understood, but it is thought to occur via direct contact with an infectious person, exposure to respiratory droplets as well as indirect contact with various contaminated surfaces (Zhang et al. 2020; Chia et al. 2020; Choi et al. 2021a; Khan et al. 2021; Chen et al. 2021). Thus, decontamination means of surfaces and closed spaces are of need. Current decontamination techniques include UV irradiation, ethylene oxide, vaporized hydrogen peroxide, ozone, moist heat incubation and microwave-generated steam (Kwok et al. 2021; Choi et al. 2021a, b; Zucker et al. 2021).

Millimeter and sub-terahertz waves at the megawatt output range are mainly used in fusion. More modest outputs of this wave range are used in dynamic nuclear polarization enhanced nuclear magnetic resonance (DNP/NMR) spectroscopy, material processing and radars (Idehara et al. 2020). These waves are generated by a Gyrotron, which is a vacuum electron tube where accelerated electrons are manipulated by a strong magnetic field into a resonator where the kinetic energy is partially converted into an electromagnetic radiation. The radiation frequency is determined mainly by the magnetic field, roughly $S \times 28$ GHz/T are obtained where S is the harmonic number (Kumar et al. 2016; Pilossof and Einat 2020).

95 GHz is a good candidate for inactivation of viruses including coronaviruses on various surfaces due to the low penetration depth of 95 GHz in materials (Hosseini et al.

✉ Matan Oren
matanor@ariel.ac.il

✉ Gabi Gerlitz
gabige@ariel.ac.il

[1] Department of Molecular Biology, Faculty of Life Sciences, Faculty of Natural Sciences, Ariel University, Kiryat Hamada, 40700 Ariel, Israel

[2] Ariel Center for Applied Cancer Research, Ariel University, Ariel, Israel

[3] Department of Electrical Engineering and Electronics, Faculty of Engineering, Ariel University, Ariel, Israel

2021) that can prevent damaging of the environment, and the ability to focus it to much better extent than microwaves. In addition, in low enough power density, 95 GHz is much less dangerous for humans then other means of decontamination such as UV irradiation and ethylene oxide (Karipidis et al. 2021), and can even be useful for cancer treatment to irradiate malignant tumors (Miyoshi et al. 2016). Here we used a 95 GHz gyrotron with ~ 10 kW output power (Pilossof and Einat 2020) to irradiate poliovirus and human coronavirus 229E. The 229E virus is responsible for upper respiratory tract infections that occasionally cause pneumonia (Hamre and Procknow 1966; Greenberg 2016) and is a common model for SARS-CoV-2. 95 GHz could inactivate the coronavirus 229E and poliovirus while disintegrating the 229E virions as detected by scanning electron microscopy (SEM). Thus, we suggest 95 GHz as a good candidate for viral decontamination.

Materials and methods

Cells

HeLa and Huh7 cells were grown in Dulbecco's modified eagle medium (DMEM) (01–056–1A, Biological industries) supplemented with 10% fetal bovine serum (FBS, 04–007–1A, Biological Industries), 0.5% penicillin–streptomycin antibiotic mix (03–031–1B, Biological Industries), and 1% L-glutamine (03–020–1B, Biological Industries) at 37 °C, 7% CO_2.

Viruses

Human coronavirus 229E (VR-740, ATCC) was propagated in Huh7 cells (Tang et al. 2005). Monolayer of cells were inoculated with the virus and incubated at 37 °C, 7% CO_2 for an hour. Then the medium was replaced with growth medium with 2.5% FBS and the cells were grown for 24 h. Following three cycles of freezing at − 80 °C and thawing at room temperature the medium containing virus was spun down to remove remaining cells, aliquoted and kept at − 80 °C until further use. Oral polio vaccine containing poliomyelitis types one and three was used without further propagation (Polio Sabin one and three, GlaxoSmithKline Biologicals S.A., Rixensart, Belgium).

Irradiation parameters

The radiated beam was of 95 GHz frequency, in a Gaussian-like beam profile (Fig. 1). The power density within the target varies between 70 and 100 W/cm^2. The radiation spot was larger than the target cup and spilled over radiation hit the surrounding surface, a Teflon sheet that was placed on a concrete surface.

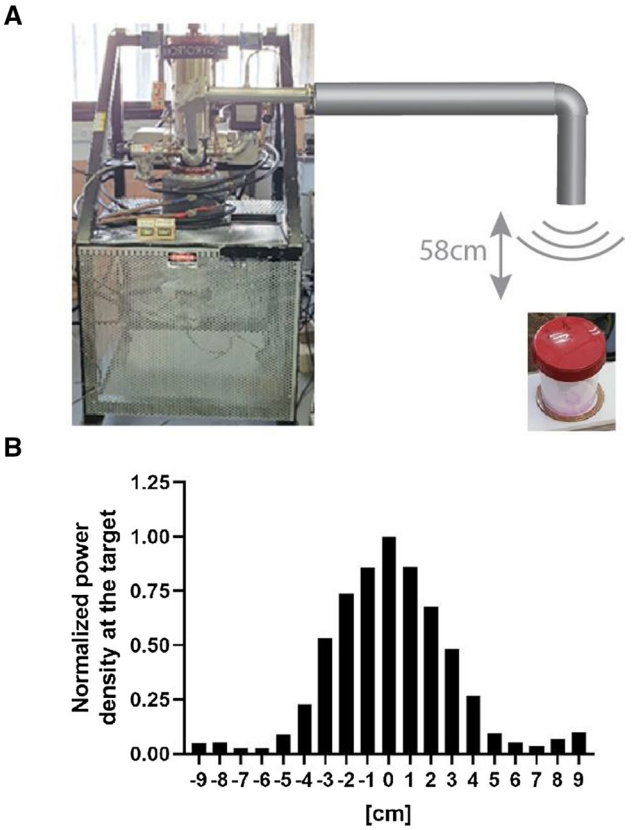

Fig. 1 The W-band gyrotron used for the irradiation of viruses. **A** Image of the W-band gyrotron used for virus irradiation and a sample cup with the virus sample in it in front of the radiation tube. **B** The W-band beam profile. The sample cup with a diameter of 4 cm was placed in the center of the beam

Plaque assay

Huh7 and HeLa cells were used for coronavirus and poliovirus, respectively (Tang et al. 2005; Burrill et al. 2013); 4.5×10^5 of cells were plated in each well of 12-well plates a day before the experiment. In the day of the experiment 70 µl of virus inoculum that contained $16.2*10^6$ of plaque-forming units (PFU)/ml of coronavirus and $4.4*10^4$ PFU/ml of poliovirus were suspended in 430 µl of DMEM and irradiated for either 0 s, 0.2 s, 0.5 s, 1 s or 2 s; 250 µl from serial dilutions of 10^{-3} to 10^{-7} for coronavirus and of 10^{-2} to 10^{-4} for poliovirus were added to cell monolayers and incubated at 37 °C, 7% CO_2 for an hour. The cell monolayer was then overlaid with 0.5% agarose in growth medium and incubated for 5 days at 37 °C, 7% CO_2. Then, cells were fixed in 2% paraformaldehyde (PFA) for 10 min, the agarose overlay was removed, and the cells were stained with 0.05% crystal violet in 20% Ethanol for 10 min. Following two washings

with water, plaques were pictured and counted in the well with highest virus dilution in which plaques were detected. Titer (PFU/ml) = well plaque count / 0.25 ml * dilution factor. GraphPad Prism 9.1.2 (GraphPad Software, San Diego, California USA) was used to analyze the data.

Microscopy

For every sample, 70 µl of coronavirus 229E solution was diluted in 430 µl of DMEM and filtered through a 0.45-µm syringe filter to remove cell debris. Three virion solutions were prepared; two filtered virion samples were irradiated as described above for either 0.1 or 1 s, while a third sample was kept as an untreated control. The irradiated samples and the control were diluted to 5 ml with DMEM and filtered through a 0.1 µm nucleopore polycarbonate track-etched filters (Whatman, Merck) held inside a 13-mm Swinnex® filter unit (Millipore, Merck) using a 5-ml syringe. The virions were fixed on the filter by pushing 3 ml of 2% glutaraldehyde in phosphate-buffered saline (PBS) two times with 15-min intervals. After 15 min from the last fixation, the syringe was removed and replaced with a syringe with 3 ml of water; 1 ml of water was pushed through three times with 5-min intervals. This was repeated with dehydration steps in ethanol in increasing concentrations of 50%, 70%, 85%, 95% and 100%. The filter was removed from the filter unit using tweezers, placed in a clean petri dish and allowed to air dry for 30 min. The dry filter was cut into quarters before coating and imaging. PBS, DMEM and Fixative solution were all filtered through a 0.45-µm syringe filter before use. All samples were imaged in a high-resolution scanning electron microscope (HRSEM) (Tescan, MAIA 3, TESCAN Ltd., Brno, Czech Republic). Platinum-coated specimens were imaged in vacuum at 5–7 kV with working distance range of 3–7 mm, magnification range of 20x–500x, pixel size (Y and X) had a range from 10 e-9 to 587 e-12 and 0.5 min to 1.36 min acquisition time per image.

Results and discussion

W-band gyrotron setup

High-power electromagnetic wave was generated by a W-band gyrotron. W-band is also known as M band in the European Union, North Atlantic Treaty Organization, and the United States military electromagnetic (EU-NATO-US ECM) frequency bands standard. The gyrotron output was coupled to an over-molded corrugated waveguide with internal diameter of 39 mm. The gyrotron output was irradiated toward a virus sample, and the main lobe angle width (3 dB) was ~ 5 degrees from the waveguide output. The virus sample, with diameter of 4 cm, was placed 58 cm from the waveguide end at the center of the main lobe (Fig. 1A). The gyrotron output mode and the propagating mode in the waveguide is a Gaussian-like mode: at the center of the sample the power density was about 100 W/cm^2 and in the edges about 70 W/cm^2 (Fig. 1B). The gyrotron output power was constant, and the pulse duration was changed from 0.2 s up to 2 s.

95 GHz waves decrease virus infectivity

Following irradiation of coronavirus 229E samples, serial dilutions of the virus were quantified for infective virions by the plaque assay (Fig. 2A, B). The inactivation was increased in an exponential manner leading to a titer decrease of almost 4 logs that corresponded to a 99.98% reduction after 2 s of irradiation. Fitting to two phase exponential decay equation was better than to one phase: R^2 of 0.98 and 0.97, respectively. The generated two phase exponential decay equation was $y = 0.5278*e^{(-16675x)} + 0.4722e^{(-2.728x)}$. We also tested the effect of 95 GHz on the infectivity of poliovirus. As seen in Fig. 2C, poliovirus was more resistant to the irradiation: 2 s of irradiation led to a titer decrease of more than 2 logs that corresponded to a reduction of 99.375%. Fitting to one phase and two-phase exponential decay equations led to a similar R^2 value of 0.89 generating the one phase decay equation $y = 1.04e^{(-1.681x)}$.

The higher resistance of poliovirus than coronavirus to irradiation may be due to the different structure of these viruses: while coronaviruses are coated by a lipid bilayer envelope (Boopathi et al. 2021), polioviruses are coated by a protein capsid that lacks any lipids (Racaniello 2016) and considered to be a highly resilient structure. The 4-log reduction in coronavirus from $1.13*10^6$ PFU to 259 PFU after 2 s of irradiation brought the remaining number of viruses close to the range of the limited infective dose for SARS-CoV-2, which was estimated to be 100 viral particles in humans and was found to be 100–630 viral particles in animal models (Karimzadeh et al. 2021).

95 GHz waves damage the virus envelope

To evaluate the effect of 95 GHz on the structure of coronavirus we used SEM analysis. SEM imaging permitted the identification of intact coronaviruses 229E that were within the expected size range of 150–200 nm in diameter, had a spherical shape and a rough envelope surface (Fig. 3A-C). When applying irradiation pulses as short as 0.1 s, some virions underwent significant morphological changes including the appearance of big holes in their envelope and the loss of their content (Fig. 3D-E). No virions were identified on the filters that were radiated for 1 s (Fig. 3F) suggesting a complete structural breakdown of most of them. Measurements of temperature changes

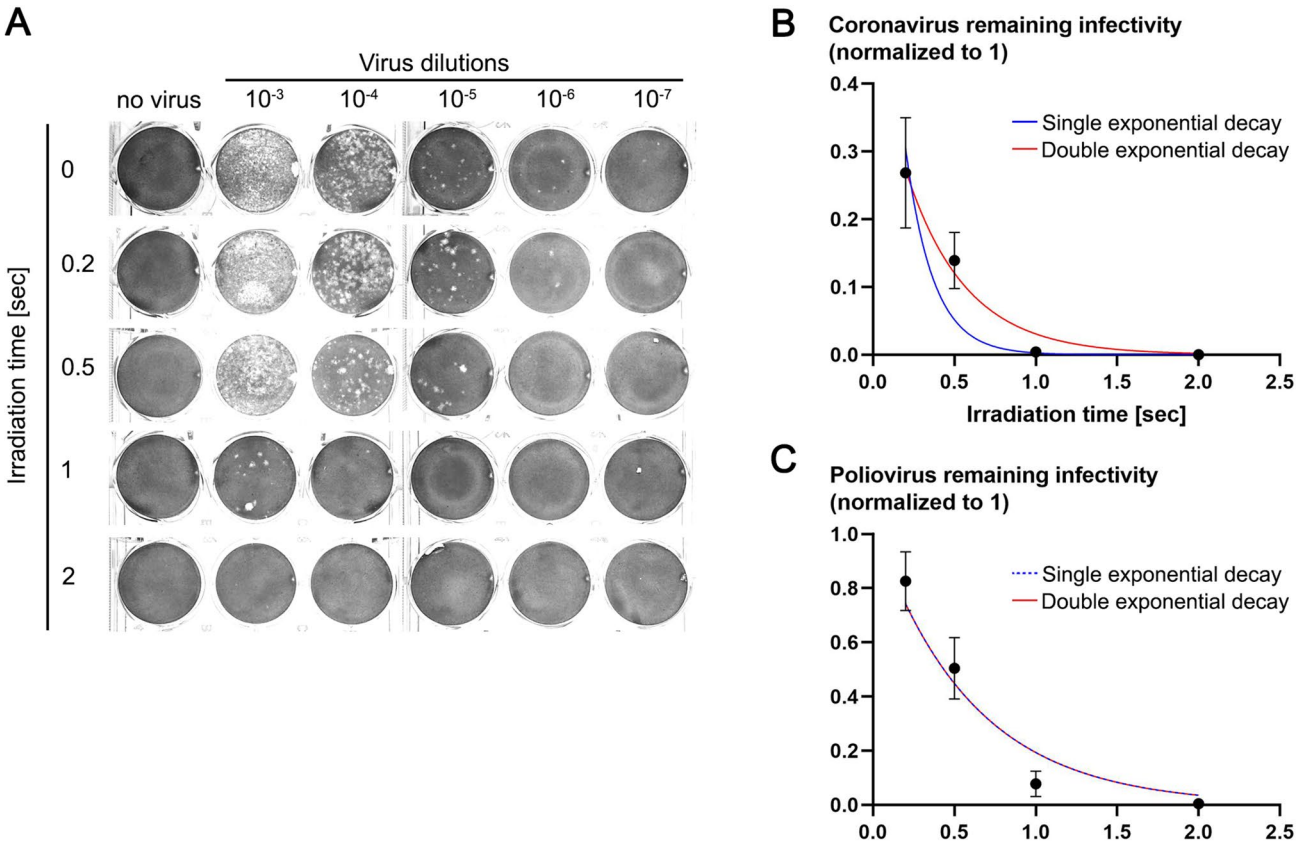

Fig. 2 Coronavirus and poliovirus infectivity rate after irradiation at 95 GHz. **A** $1.13*10^6$ plaque-forming units (PFU) of coronavirus 229E were irradiated at 95 GHz for the indicated time periods and quantified by the plaque assay. The limit of detection for coronavirus was 200 PFU. **B** Averages of coronavirus 229E infectivity rate after 95 GHz irradiation. The results are shown as means ± standard error (SE) for three independent experiments. Blue line indicates single exponential decay function, while red line indicates double exponential decay function. **C** Averages of poliovirus infectivity rate after 95 GHz irradiation. The results are shown as means ± SE for four independent experiments. Blue dashed line indicates single exponential decay function, while red line indicates double exponential decay function. The limit of detection for poliovirus was 20 PFU

in the irradiated sample cup were taken and showed an increase in temperature up to 100 ºC at the time range of 0.2–0.7 s of irradiation. Taking together the rapid temperature changes, the changes in the virus structure (Fig. 3) and the increased sensitivity to irradiation of coronavirus compared to poliovirus (Fig. 2) led us to suggest that the viruses were damaged by the elevated temperatures. The viruses could be heated directly and indirectly by heated water around them. The rapid heating and cooling afterward, which did not harm the polypropylene sample cup, may also have accelerated the damage to the viruses. Significantly, the inactivation exposure time of coronavirus by 95 GHz was faster than similar inactivation rates by UV-C and conventional heating (Abraham et al. 2020; Sabino et al. 2020; Storm et al. 2020; Gidari et al. 2021; Biryukov et al. 2021).

Conclusion

The presented results show that an energy density of 100 W/cm^2 at 95 GHz for 2 s caused a coronavirus titer reduction of 4 logs, reducing it very close to the minimal infective dose for SARS-CoV-2 in humans. This type of sterilization has the benefits of being faster and better directed to a specific surface than UV-based or conventional thermal sterilization. In principle, it is possible to illuminate a large surface and perform fast sterilization of large areas in a few seconds. It is also possible to seal the contaminated objects in a sealed container and perform sterilization in a standoff manner. In this manner, there is no direct touch or exposure of the operating persons to the pathogens. In addition to surface decontamination, this approach may be used to disinfect wastewater or other sources of microbial contaminated water. On the other

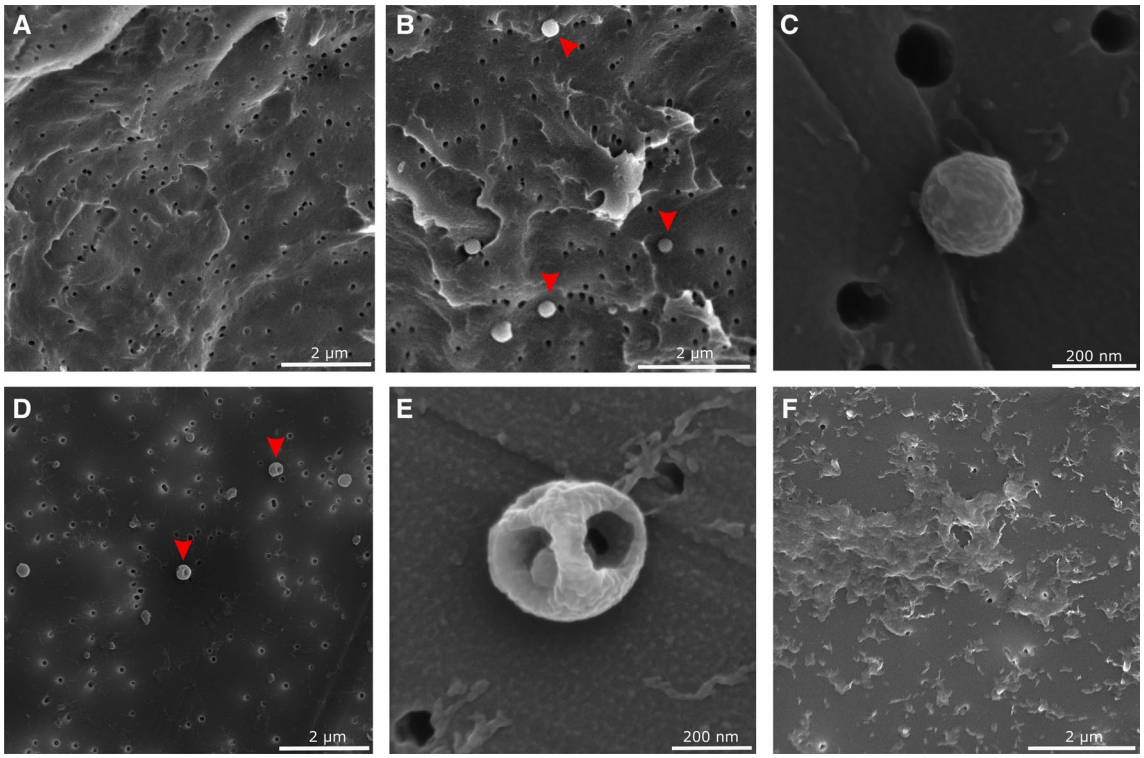

Fig. 3 Scanning electron microscopy (SEM) analysis of coronavirus 229E structure after irradiation at 95 GHz. **A** 0.1-µm filter with no sample shows clear surface with pores easily visible. **B** Unirradiated coronavirus 229E virions on filter. Red arrows mark some of the virions. **C** An intact coronavirus 229E virion of approximate 200 nm diameter. **D**, **E** Coronavirus 229E virions after 0.1 s irradiation. Virion envelope appears damaged. Red arrows mark damaged virions. **F** Filter with sample after 1 s irradiation. No virions are observed

hand, the power density is significant, and some surfaces might not tolerate it, although the rapid and transient temperature changes may prevent damage to materials that are considered heat-sensitive such as polypropylene cups. We used a facility that operates in 95 GHz but the optimal frequency for virus decontamination at the millimeter waves range is still to be assessed. Overall, these results suggest for the first time that 95 GHz waves may be an easy and fast method to decontaminate objects from various viruses.

Acknowledgments We thank Ella Sklan (Tel Aviv University, Tel Aviv, Israel) for providing Huh7 cells.

Author contributions Conceptualization, funding acquisition and supervision were performed by Moshe Einat, Matan Oren and Gabi Gerlitz. Investigation was performed by Lukasz S. Kaczmarczyk, Katherine S. Marsay, Sergey Shevchenko, Moritz Pilossof and Nehora Levi. Visualization was performed by Lukasz S. Kaczmarczyk, Katherine S. Marsay, Sergey Shevchenko, Moritz Pilossof, Moshe Einat, Matan Oren and Gabi Gerlitz. Katherine S. Marsay, Moritz Pilossof, Moshe Einat, Matan Oren and Gabi Gerlitz were responsible for writing—original draft. Lukasz S. Kaczmarczyk, Katherine S. Marsay, Moshe Einat, Matan Oren and Gabi Gerlitz were responsible for writing—review & editing.

Funding This work was funded by Ariel University.

Declarations

Conflicts of interest The authors declare that they have no conflict of interest.

References

Abraham JP, Plourde BD, Cheng L (2020) Using heat to kill SARS-CoV -2. Rev Med Virol 30:e2115. https://doi.org/10.1002/rmv.2115

Atzrodt CL, Maknojia I, McCarthy RDP et al (2020) A Guide to COVID-19: a global pandemic caused by the novel coronavirus SARS-CoV-2. FEBS J 287:3633–3650. https://doi.org/10.1111/febs.15375

Biryukov J, Boydston JA, Dunning RA et al (2021) SARS-CoV-2 is rapidly inactivated at high temperature. Environ Chem Lett 19:1773–1777. https://doi.org/10.1007/s10311-021-01187-x

Boopathi S, Poma AB, Kolandaivel P (2021) Novel 2019 coronavirus structure, mechanism of action, antiviral drug promises and rule out against its treatment. J Biomol Struct Dyn 39:3409–3418. https://doi.org/10.1080/07391102.2020.1758788

Burrill CP, Strings VR, Andino R (2013) Poliovirus: generation, quantification, propagation, purification, and storage. Curr Protoc Microbiol. https://doi.org/10.1002/9780471729259.mc15h01s29

Chen B, Jia P, Han J (2021) Role of indoor aerosols for COVID-19 viral transmission: a review. Environ Chem Lett 19:1953–1970. https://doi.org/10.1007/s10311-020-01174-8

Chia PY, Coleman KK, Tan YK et al (2020) Detection of air and surface contamination by SARS-CoV-2 in hospital rooms of infected patients. Nat Commun 11:2800. https://doi.org/10.1038/s41467-020-16670-2

Choi H, Chatterjee P, Coppin JD et al (2021a) Current understanding of the surface contamination and contact transmission of SARS-CoV-2 in healthcare settings. Environ Chem Lett. https://doi.org/10.1007/s10311-021-01186-y

Choi H, Chatterjee P, Lichtfouse E et al (2021b) Classical and alternative disinfection strategies to control the COVID-19 virus in healthcare facilities: a review. Environ Chem Lett 19:1945–1951. https://doi.org/10.1007/s10311-021-01180-4

Dai H, Han J, Lichtfouse E (2021) Smarter cures to combat COVID-19 and future pathogens: a review. Environ Chem Lett 19:2759–2771. https://doi.org/10.1007/s10311-021-01224-9

Gidari A, Sabbatini S, Bastianelli S et al (2021) SARS-CoV-2 Survival on Surfaces and the Effect of UV-C Light. Viruses 13:408. https://doi.org/10.3390/v13030408

Greenberg S (2016) Update on human rhinovirus and coronavirus infections. Semin Respir Crit Care Med 37:555–571. https://doi.org/10.1055/s-0036-1584797

Hamre D, Procknow JJ (1966) A new virus isolated from the human respiratory tract. Exp Biol Med 121:190–193. https://doi.org/10.3181/00379727-121-30734

Hosseini N, Khatun M, Guo C et al (2021) Attenuation of several common building materials: millimeter-wave frequency bands 28, 73, and 91 GHz. IEEE Antennas Propag Mag. https://doi.org/10.1109/MAP.2020.3043445

Idehara T, Sabchevski SP, Glyavin M, Mitsudo S (2020) The gyrotrons as promising radiation sources for THz sensing and imaging. Appl Sci 10:980. https://doi.org/10.3390/app10030980

Karimzadeh S, Bhopal R, Nguyen Tien H (2021) Review of infective dose, routes of transmission and outcome of COVID-19 caused by the SARS-COV-2: comparison with other respiratory viruses. Epidemiol Infect 149:e96. https://doi.org/10.1017/S0950268821000790

Karipidis K, Mate R, Urban D et al (2021) 5G mobile networks and health-a state-of-the-science review of the research into low-level RF fields above 6 GHz. J Expo Sci Environ Epidemiol. https://doi.org/10.1038/s41370-021-00297-6

Khan AH, Tirth V, Fawzy M et al (2021) COVID-19 transmission, vulnerability, persistence and nanotherapy: a review. Environ Chem Lett. https://doi.org/10.1007/s10311-021-01229-4

Kumar N, Singh U, Bera A, Sinha AK (2016) A review on the sub-THz/THz gyrotrons. Infrared Phys Technol 76:38–51. https://doi.org/10.1016/j.infrared.2016.01.015

Kwok CS, Dashti M, Tafuro J et al (2021) Methods to disinfect and decontaminate SARS-CoV-2: a systematic review of *in vitro* studies. Ther Adv Infect 8:204993612199854. https://doi.org/10.1177/2049936121998548

Miyoshi N, Idehara T, Khutoryan E et al (2016) Combined hyperthermia and photodynamic therapy using a sub-THz gyrotron as a radiation source. J Infrared Milli Terahz Waves 37:805–814. https://doi.org/10.1007/s10762-016-0271-z

Pilossof M, Einat M (2020) High-average-power second harmonic *W* -band gyrotron with room-temperature solenoid. IEEE Trans Electron Devices 67:1804–1807. https://doi.org/10.1109/TED.2020.2971653

Racaniello V (2016) Poliovirus. In: Reiss CS (ed) Neurotropic Viral Infections. Springer International Publishing, Cham, pp 1–26

Sabino CP, Sellera FP, Sales-Medina DF et al (2020) UV-C (254 nm) lethal doses for SARS-CoV-2. Photodiagn Photodyn Ther 32:101995. https://doi.org/10.1016/j.pdpdt.2020.101995

Sallard E, Halloy J, Casane D et al (2021) Tracing the origins of SARS-COV-2 in coronavirus phylogenies: a review. Environ Chem Lett 19:769–785. https://doi.org/10.1007/s10311-020-01151-1

Storm N, McKay LGA, Downs SN et al (2020) Rapid and complete inactivation of SARS-CoV-2 by ultraviolet-C irradiation. Sci Rep 10:22421. https://doi.org/10.1038/s41598-020-79600-8

Tang BSF, Chan K-H, Cheng VCC et al (2005) Comparative host gene transcription by microarray analysis early after infection of the Huh7 cell line by severe acute respiratory syndrome coronavirus and human coronavirus 229E. J Virol 79:6180–6193. https://doi.org/10.1128/JVI.79.10.6180-6193.2005

Zhang R, Li Y, Zhang AL et al (2020) Identifying airborne transmission as the dominant route for the spread of COVID-19. Proc Natl Acad Sci USA 117:14857–14863. https://doi.org/10.1073/pnas.2009637117

Zhu N, Zhang D, Wang W et al (2020) A novel coronavirus from patients with pneumonia in China, 2019. N Engl J Med 382:727–733. https://doi.org/10.1056/NEJMoa2001017

Zucker I, Lester Y, Alter J et al (2021) Pseudoviruses for the assessment of coronavirus disinfection by ozone. Environ Chem Lett 19:1779–1785. https://doi.org/10.1007/s10311-020-01160-0